Engenharia Agrícola

ISSN: 1809-4430 (on-line)

www.engenhariaagricola.org.br

Scientific Paper
Doi: http://dx.doi.org/10.1590/1809-4430-Eng.Agric.v42n5e20220043/2022

THERMAL IMAGING FOR STRESS ASSESSMENT IN RICE CULTIVATION DRIP-IRRIGATED WITH SALINE WATER

Luana C. Menegassi[1*], Vinicius C. Benassi[1], Lucas R. Trevisan[1], Fabrício Rossi[2], Tamara M. Gomes[2]

[1*]Corresponding author. Department of Biosystems Engineering, Luiz de Queiroz College of Agriculture, University of São Paulo/Piracicaba - SP, Brazil. E-mail: luana.menegassi@usp.br | ORCID ID: https://orcid.org/0000-0001-7626-0616

KEYWORDS

Localized irrigation, special rice, remote sensing, canopy temperature.

ABSTRACT

Lowland rice is traditionally irrigated by flood systems, demanding high water consumption. Localized irrigation by subsurface dripping is proposed as an alternative, in addition to the replacement of the source of water intended for human consumption with another of lower quality, such as saline water. However, plants can be affected by saline and/or water stress in both conditions, and the use of thermal imaging emerges as a tool to assess the plant status. In this context, this study aimed to identify the stress of subsurface drip-irrigated arborio rice under different salt concentrations and soil moisture by thermographic images. The design consisted of randomized blocks in a (2×4)+2 factorial with three replications, totaling 30 experimental plots. Soil solution salinity was assessed by electrical conductivity. The thermal images were processed by an algorithm to determine the normalized relative canopy temperature (NRCT) index at different crop development stages. Saline stress was identified by the NRCT index, with higher sensitivity of plants at the flowering stage with a rebalance over time, confirmed at grain filling and harvest stages.

INTRODUCTION

Rice is one of the main grains present in the Brazilian diet, with significant national production. In Brazil, the planted area in 2021 reached 1.66 million hectares and grain production was 11.38 million tons, with productivity of 6,832.00 kg ha^{-1} (CONAB, 2022). Rice cultivation in Brazil is predominantly carried out under flood irrigation systems. Upland planting corresponds to 25% of the cultivated area and 10% of production, while flooded rice accounts for 75% of the cultivated area and 90% of production (ANA, 2020).

Production in the flood system requires an average water volume from 6 to 12 thousand m^3 ha^{-1} for an irrigation period of 80 to 100 days (SOSBAI, 2018), with an average of 8.9 thousand m^3 ha^{-1} (ANA, 2020). The low efficiency of this system is related to losses by evaporation, percolation, and lateral flow, which corresponds to 44% of the total volume of water used in paddy fields (Chapagain & Hoekstra, 2011).

Thus, practices and technologies to improve water use efficiency in rice cultivation are necessary for this scenario of water scarcity. Localized irrigation consists of a method with better water use efficiency than the flood system (Sharda et al., 2017), as it applies water at a high frequency and low volume. Additionally, the source of water intended for irrigation should consist of lower quality water, such as saline water, whenever possible. Thus, better quality water can be conserved for nobler uses, such as human supply.

However, the presence of salts and soil moisture reduction in rice cultivation can lead to physiological and biochemical changes in plants, affecting production (Frukh et al., 2020; Mekawy et al., 2015). The incorporation of technologies in the field, such as remote sensing, has been increasingly applied to assess the crop status, thus helping the producer in decision-making regarding the management to be adopted (Khanal et al., 2017).

[1] Department of Biosystems Engineering, Luiz de Queiroz College of Agriculture, University of São Paulo/Piracicaba - SP, Brazil .
[2] Department of Biosystems Engineering, Faculty of Animal Science and Food Engineering, University of São Paulo/Pirassununga - SP, Brazil.

Area Editor: Fernando França da Cunha
Received in: 3-23-2022
Accepted in: 8-31-2022

Remote sensing, incorporated in precision agriculture, refers to obtaining data without physical contact with the object of study (Shanmugapriya et al., 2019). This technology associated with advances in computational capacity, allows the collection of data and the extraction of crucial information for crop management with a temporal resolution (Sishodia et al., 2020). The use of images in this segment has shown good results in the monitoring of factors, such as nitrogen status (Li et al., 2014), water stress (Khorsandi et al., 2018), and pest and disease incidence (Mahlein et al., 2013).

The use of images for remote sensing is subject to the availability of cameras that operate at different bands of the electromagnetic spectrum. Indices are commonly used in agricultural applications to assess the development of a crop by associating values measured at different bands of the electromagnetic spectrum (Liu et al., 2021), such as the thermographic camera, capturing images through radiation in the thermal infrared range (0.8 to 13 μm), emitted by the object under study, and the higher the radiation, the higher the object temperature (Elsayed et al., 2021). Therefore, thermal images are important tools in the development of indices for stress assessment (Gerhards et al., 2019) and can help in monitoring the physiological changes of plants irrigated with saline water with great repeatability and low cost compared to traditional methods (Kondo et al., 2021).

The normalized relative canopy temperature (NRCT) index, developed by Elsayed et al. (2015), has been used as an indicator of crop water stress determined by thermal imaging (Elsayed et al., 2017; Elsayed et al., 2021). The main advantage is the use of characteristics present exclusively in a data source, without the need for additional measurements, such as weather variables (Idso et al., 1981).

Thus, this research aimed to assess the potential of thermal imaging in stress monitoring in drip irrigated rice plants at different salinity doses measured by the electrical conductivity of the soil solution under two moisture conditions by determining the NRCT index and its relationship with canopy water status.

MATERIAL AND METHODS

Study area and experimental design

The experiment was carried out in a protected environment with an area of 210 m^2 at the School of Animal Science and Food Engineering (FZEA/USP) of the Department of Biosystems Engineering, Pirassununga-SP, Brazil, at an altitude of 627 m and geographic coordinates 21°59′ S and 47°25′ W. The mean air temperature was monitored through the daily reading of the digital weather station located in the central area of the greenhouse. The global solar radiation was obtained by an LI-COR LI-200 pyranometer installed at the weather station.

The experiment was randomized in blocks in a (2×4)+2 (two controls) factorial scheme, with three replications, consisting of two soil moisture conditions (saturate–SAT and field capacity–FC) and four salinity doses, referring to electrical conductivity (EC): 1 dS m^{-1} (1EC), 2 dS m^{-1} (2EC), 3 dS m^{-1} (3EC), and 4 dS m^{-1} (4EC) (Figure 1). The control treatments consisted of irrigation with potable water, with soil moisture at field capacity (0EC–FC), and irrigation with potable water, with moisture close to soil saturation (0EC–SAT). The experimental plots totaled 30 units consisting of fiberglass boxes with 1 m^2 of surface area and 500 L of volume.

Block 1	Block 2	Block 3	Block 4
T3	T2	T5	T4
T1	T4	T7	T8
T5	T6	T8	T3
T2	T7	T9	T5
T8	T10	T1	T2
T9	T3	T10	T6
T6	T9	T2	T7
T10	T8	T4	T9
T4	T1	T6	T10
T7	T5	T3	T1

Treatment	Salinity dose	Soil moisture
T1	0EC	Field capacity
T2	0EC	Saturate
T3	1dS m^{-1} (1EC)	Field capacity
T4	1dS m^{-1} (1EC)	Saturate
T5	2dS m^{-1} (2EC)	Field capacity
T6	2dS m^{-1} (2EC)	Saturate
T7	3 dS m^{-1} (3EC)	Field capacity
T8	3 dS m^{-1} (3EC)	Saturate
T9	4 dS m^{-1} (4EC)	Field capacity
T10	4 dS m^{-1} (4EC)	Saturate

FIGURE 1. Experimental design. Electrical conductivity- EC.

Sowing and fertilization

Sowing was carried out on August 24, 2020, with an inter-row spacing of 0.17 m, a density of 50 seeds m^{-1}, and four rows per plot. The special arborio rice of the cultivar IAC 301 (used in Italian cuisine) was used. The cultivation cycle was 133 days.

All plots received planting fertilization via fertigation, based on the results of soil analysis. A dose of 60 kg ha^{-1} of P_2O_5 and 30 kg ha^{-1} of nitrogen (N) was applied to all treatments, 70 kg ha^{-1} of K_2O was applied to treatments T1, T2, and T3, and 20 kg ha^{-1} of K_2O was applied to the other treatments. Nitrogen and potassium were split into four applications with a daily frequency, while phosphorus was applied in a single dose. The sources were calcium nitrate (15.5% N and 19% Ca) and potassium nitrate (12% N, 43% K_2O, 1% S, and 1% Mg), with solubilities in water at 20 °C of 310 and 300 g L^{-1}, respectively, and phosphoric acid (H_3PO_4).

Topdressing fertigation was performed in all treatments from seedling emergence, comprising the vegetative and early reproductive stages (Crusciol et al., 2016). A dose of 100 kg ha^{-1} of N and 90 kg ha^{-1} of K_2O was applied via fertigation. The sources consisted of calcium nitrate and potassium nitrate, split into five applications with a weekly frequency.

Saline water, irrigation, and soil solution

The saline solution was prepared in a 500 liter water tank. The useful volume for calculating the concentration was 330 liters. The solution was prepared for the upper electrical conductivity condition (4 dS m^{-1}), using a concentration of 2.30 g L^{-1} of salt (sodium chloride).

The subsurface drip irrigation system was adopted. Each plot had four 1 m long drip lines buried at a depth of 0.15m (Sidhu et al., 2019), with drippers spaced at 0.15 m from each other and 0.20 m between irrigation lines. Netafim Aries integrated non-pressure compensating drippers with anti-siphon, a flow rate of 1.6 L h^{-1}, and working pressure of 1.5 bar.

The treatments were individualized by solenoid valves, one for each treatment, operated by a Hunter® Pro-C controller panel, and two motor pumps, one for each water source (potable and saline water). The output of each motor pump consisted of a disc filter for solid retention and manometers for pressure control. Each treatment received a hydrometer to control the water volume, in addition to a pressure regulator of 1.7 bar.

A water application uniformity test was carried out before the beginning of the experiment to determine the Christiansen uniformity coefficient in each plot, with volume collection of all emitters, whose average value was 97%, which is considered excellent. Phosphorus for fertilization was applied by fertigation as phosphoric acid, thus favoring the cleaning of drippers to prevent clogging despite the short time of use.

Irrigation management was carried out based on soil moisture determination by tensiometers installed in the central part of the experimental plot at a depth of 0.20 m, with three replications per treatment (blocks 1, 3, and 4), with two-day irrigation frequencies. The tension values obtained by tensiometer readings were transformed to moisture by the soil-water retention curve at a depth of 0.20 m constructed at the Laboratory of the Department of Natural Resources and Environmental Protection of the Center for Agrarian Sciences at UFSCar. The data obtained in the laboratory were adjusted by the van Genuchten (1980) model, using the RETC software (van Genuchten et al., 1991) version 6.00, which provided the moisture values adopted for field capacity (9 kPa) and saturation to define the water depths as a function of the adopted treatments.

Porous capsule soil solution extractors were installed centrally in each plot at a depth of 0.20 m and 0.10 m from the tensiometers to monitor the electrical conductivity (EC) of the soil solution. The solution was collected monthly after applying a vacuum using a 60 mL syringe, comprising the tillering, flowering, grain filling, and harvesting stages. After collection, the solution samples were analyzed at the Laboratory of Biosystems of FZEA-USP for EC measurement using a benchtop conductivity meter.

Thermal imaging

Thermal images to determine canopy temperature were taken using a FLIR E60 handheld thermographic camera, with a resolution of 320×240 pixels, thermal sensitivity <0.05 °C, and a field of view of 25°×19°. This equipment can capture radiation emissions with a wavelength in the infrared and generate an image based on the intensities of this energy emitted from the object so that each pixel of the image represents the intensity measured at that point.

The camera emissivity was set to 0.95 (Glenn, 2012). The camera was positioned perpendicularly to the central part of the plot using a holder to ensure a height of 2.0 m from the ground and, therefore, better image framing and standardization. The camera positioning allowed the assessment of an area of 0.25 m^2 in the central part of each plot.

Collections were carried out between 30 and 130 days after seedling emergence, always in the morning, until 11:00 am, in order to avoid reaching the highest temperatures of the day, together with the soil solution collection. The assessment dates were October 21, 2020 (tillering stage), November 18, 2020 (flowering stage), December 16, 2020 (grain filling stage), and January 4, 2021 (harvest).

The processing of thermal images was performed using the FLIR Tools software, which provided emissivity, capture distance, ambient temperature (°C), and relative humidity (%), determined at the image capture time. Subsequently, an algorithm in Python language was used to segment the image and remove the background that does not correspond to the plant material. For this, a blurring filter was used to accentuate the contours present in the image so that the background could be later removed together with the lower and upper levels of the maximum and minimum temperature, which are at 2.5% from the extremes, leaving only temperature values between 2.5 and 97.5% of each image (Struthers et al., 2015). This method removes abnormal colder and warmer leaf temperatures due to the leaf angle effect (Jones et al., 2009).

Then, the maximum (Tmax), minimum (Tmin), and mean (Tmean) temperature of each image was determined, with the mean temperature being calculated by the arithmetic mean present in the temperature matrix obtained with the removal of the background and thermal extremes through the segmentation by the Python language.

Plant canopy status assessment

The rice plant canopy temperature data, obtained by processing the thermal images at each crop development stage, allowed the determination of the normalized relative canopy temperature (NRCT) index, adapted from Elsayed et al. (2015) for thermal cameras (Equation 1).

$$NRCT = \frac{Tmean - Tmi}{Tmax - Tmin} \quad (1)$$

Where:

Tmean is the actual temperature measured in the canopy and Tmin and Tmax are the lowest and highest temperatures measured in the entire experimental plot, respectively. NRCT values range from 0 to 1, with more severe stress when values are close to 1 (Elsayed et al., 2015).

The canopy water content (CWC) was determined at harvesting time by [eq. (2)] (Elsayed et al., 2015).

$$CWC(\%) = \frac{FBW - D}{FBW} \quad (2)$$

Where:

FBW and DBW correspond to the fresh and dry biomass weight, respectively. The useful area considered for evaluation was 0.5 m^2, with the manual harvest of plants and subsequent separation of grains and biomass. The biomass was dried in a forced-air circulation oven at 65 °C until constant weight. Subsequently, DBW was determined in a precision scale and the data were transformed into kg ha^{-1}.

Data analysis

Analyses of variance were performed for the variables EC of soil solution and NRCT for each crop development stage. The means were compared between treatments by Tukey's test in cases of significant differences ($p<0.05$). An analysis of variance was performed in the harvest for the variable CWC and regression analysis between NRCT x CWC. The analyses were performed in the software Sisvar 5.3 (Ferreira, 2019) and Minitab version 18.

RESULTS AND DISCUSSION

Climate variables and irrigation

Figure 2 shows the average values of air temperature and global solar radiation obtained during the experiment, especially on the days that the thermal images were collected. Similar behavior is observed between temperature and solar radiation, whose temperature variation was 13 to 40 °C. The average solar radiation was 642.52 w m^{-2}, and the lowest value was recorded at the end of September (74.05 w m^{-2}, September 20, 2020) and the highest value was recorded in November (716.57 w m^{-2}, November 23, 2020).

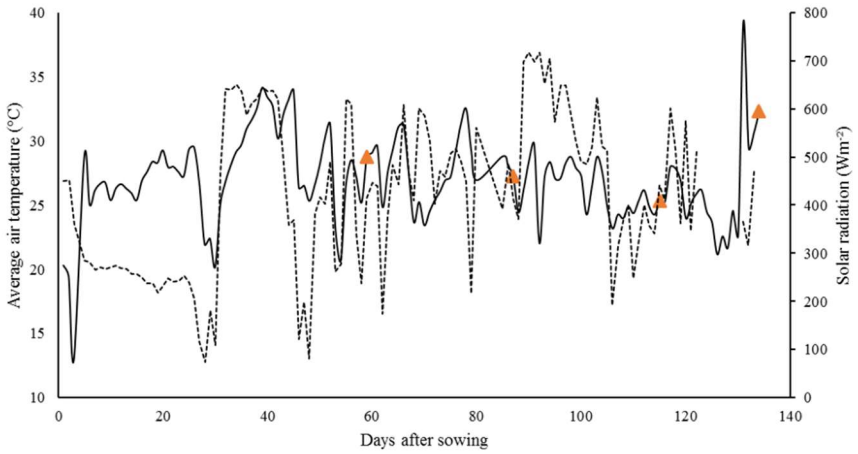

FIGURE 2. Daily averages of air temperature (solid line) and global solar radiation (dotted line), from 08/24/2020 to 01/04/2021. The triangles represent the dates thermal images were collected.

Studies have suggested that the optimal temperature during the vegetative stage is 28.4 °C, with minimum and maximum limits of 16.4 and 35.3 °C, respectively. The grain filling stage has an optimal temperature of 24.2 °C, with minimum and maximum limits of 20.7 to 31.3 °C, respectively (Sánchez et al., 2014). A value of 33 °C has been identified as the threshold for spikelet sterility (Bheemanahalli et al., 2016). A positive correlation is observed between solar radiation and rice grain production due to improved leaf photosynthetic performance, with increased biomass production and, consequently, grain yield (Arai-Sanoh et al., 2020). Thus, high values of solar radiation may alter the plant response under water stress and, consequently, the canopy temperature, as verified by Agam et al. (2013), who found a high water stress index of olive trees, with a null effect in well-hydrated trees.

Soil tension was maintained within the management range adopted for the two soil moisture conditions throughout the cycle, and treatments with soil moisture at saturation presented average tension values of 1.22±0.78 kPa and field capacity of 6.06±4.30 kPa.

Figure 3 shows the water depths of the water sources applied to each treatment. FC showed an average water saving of 64% compared to the moisture at SAT, and the highest water depth occurred in the treatment 0EC at SAT (956 mm) and the lowest water depth was observed for the treatment 2EC at FC (485 mm).

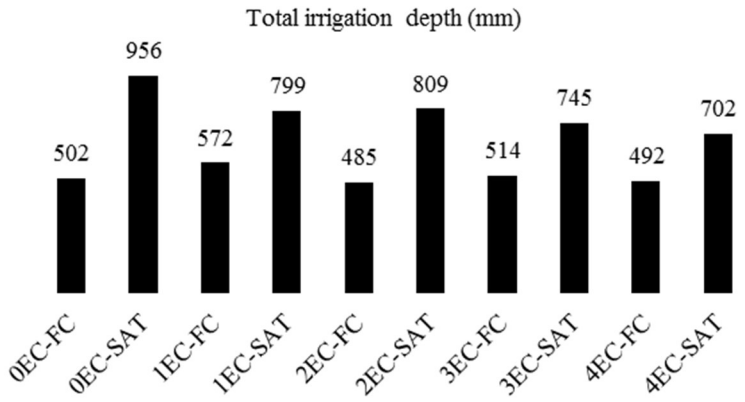

FIGURE 3. Total irrigation depth (mm) as a function of electrical conductivity dose (EC) and humidity (saturate – SAT and field capacity – FC). 0EC- 0 dS m^{-1}; 1EC- 1dS m^{-1}; 2EC- 2dS m^{-1}; 3EC- 3 dS m^{-1}; 4EC- 4 dS m^{-1}.

Coltro et al. (2017) found values of 1,400 mm for rice cultivation irrigated by flood and 900 mm by drip irrigation, whereas Sharda et al. (2017) reported values from 860 to 904 mm for drip irrigation, values close to those of this study in the comparison within localized irrigation. Both report water savings of 42% (Coltro et al., 2017) and 40% (Sharda et al., 2017) compared to the flood system, without compromising grain yield.

Soil solution electrical conductivity

Soil solution EC showed a difference during the crop development stages. Tillering, grain filling, and harvesting stages (Table 1) showed an interaction between dose and soil moisture, while soil solution EC was altered by the doses at the flowering stage (Table 2).

TABLE 1. Electrical conductivity (EC) of the soil solution according to the doses and moisture content (saturate – SAT and field capacity- FC), during the crop development stages.

		Salinity doses					
Stages	Soil moisture	0EC	1EC	2EC	3EC	4EC	VC (%)
Tillering	FC	0.42Ba	0.53Ba	0.47Bb	0.77Ba	4.07Ab	25.53
	SAT	0.34Ca	0.91BCa	1.52Ba	1.34BCa	5.64Aa	
Grain filling	FC	0.50Ca	1.02Ca	1.57Ca	2.82Ba	4.89Aa	21.79
	SAT	0.47Ca	1.17BCa	1.84Ba	1.84Bb	3.90Ab	
Harvesting	FC	0.51Da	1.02CDa	1.51BCa	2.11Ba	4.48Aa	18.17
	SAT	0.45Ca	1.16BCa	1.93Ba	1.79Ba	3.64Ab	

0 EC - 0 dS m^{-1}; 1 EC - 1dS m^{-1}; 2 EC - 2dS m^{-1}; 3 EC - 3 dS m^{-1}; 4 EC - 4 dS m^{-1}; VC - coefficient of variation. Means followed by different lowercase letters in the column and uppercase letters in the row are statistically different by Tukey's test ($p<0.05$).

Soil solution EC during tillering was higher at saturation moisture for the 2EC and 4EC doses. EC values in the soil solution were higher regardless of the moisture condition for the dose 4EC and the other doses were similar to the control (0EC), for moisture at field capacity, whereas at saturation were 1EC and 3EC.

An opposite behavior to that presented during tillering was observed at grain filling and harvesting when comparing the moistures within each EC dose, with higher values for the increment of salinity doses at the FC condition. It may be associated with the drip irrigation system, which concentrated the strip moisture in the surface layers under the adopted spacing condition, while water depth at SAT favored salt dissolution to deeper layers, thus reducing their contents on the surface (Zamann et al., 2018).

During grain filling, the 1EC dose was similar to the control at saturation moisture and 1EC and 2 EC were similar to the control at FC. In contrast, the 1EC dose was similar to the control at harvest for both soil moistures (FC and SAT).

The highest soil solution EC value during the beginning of flowering (Table 2) was observed for the 4EC dose. Except for 3EC, the other doses did not differ from the control. Thus, the 4EC dose for both moisture ranges presented the highest soil solution EC values regardless of the vegetative development stage.

TABLE 2. Electrical conductivity (EC) of the soil solution at the beginning of flowering.

Salinity doses	EC
0EC	0.57c
1EC	0.97bc
2EC	1.11bc
3EC	1.70b
4EC	4.08a
VC (%)	32.35

0EC- 0 dS m^{-1}; 1EC- 1dS m^{-1}; 2EC- 2dS m^{-1}; 3EC- 3 dS m^{-1}; 4EC- 4 dS m^{-1}; VC: coefficient of variation. Means followed by different letters are statistically different by Tukey's test ($p<0.05$).

The salinity dynamics in the soil solution can be observed during the development stages. The increased soil EC during the crop cycle is expected due to the higher input of salts via irrigation. Silva (2002) found a similar behavior, with soil solution EC varying over time. This author also observes that the concentration distribution in the soil solution is slower for values lower than 4 dS m^{-1}.

Rice is considered a moderately salinity-sensitive crop, tolerating an EC of up to 3.3 dS m^{-1} in the soil solution and up to 2.0 dS m^{-1} in the irrigation water without compromising its productive potential (Ayers & Westcost, 1999). Therefore, saline waters with EC values of up to 3 dS m^{-1} can replace higher-water quality during the tillering stage due to the dynamics of salinity in the soil solution, but this value changes to 2 dS m^{-1} during flowering. Water with EC values of up to 2 and 1 dS m^{-1} can be used at FC and saturation, respectively, during the grain filling stage. Therefore, higher-quality water sources can be partially or totally replaced by lower-quality water sources in irrigation systems in regions with water scarcity or the potential for reuse water.

Normalized relative canopy temperature and canopy water content

Figure 4 shows the thermal images before the NRCT determination. The crop canopy is represented by colors that correspond to the coldest temperatures and the background of the image (soil) is represented by colors that correspond to the warmest temperatures. The average temperature variation presented similar values for the images, with a minimum of 23.2 °C for the T8 treatment and a maximum of 24.6 °C for the T5 treatment. It occurred because the average temperature was calculated in only one of the leaves. Thus, the use of image processing through the algorithm developed by this research promoted the removal of the background and enabled the calculation of the NRCT index using only pixels referring to the plant canopy.

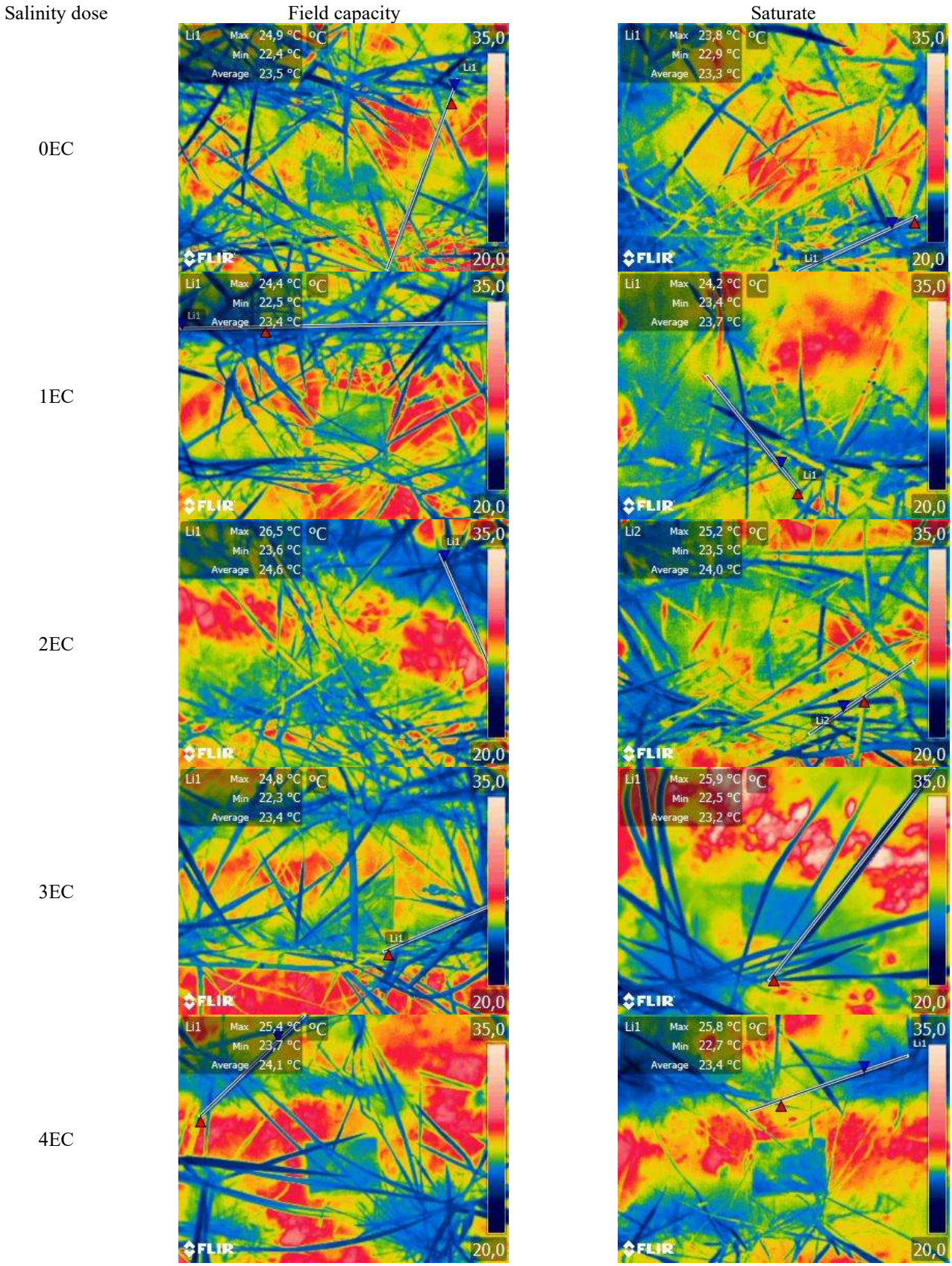

FIGURE 4. Thermal images of special rice irrigated with saline doses at 130 days after sowing. Electrical conductivity- EC; 0EC- 0 dS m^{-1}; 1EC- 1dS m^{-1}; 2EC- 2dS m^{-1}; 3EC- 3 dS m^{-1}; 4EC- 4 dS m^{-1}.

NRCT was changed by doses during the tillering, flowering, and grain filling stages (Table 3), and interaction between dose and moisture was observed at harvest (Table 4). NRCT presented different behaviors at each development stage relative to the salinity dose, unlike soil solution EC, which increased with salt addition (Tables 1 and 2).

TABLE 3. The normalized relative canopy temperature (NRCT) index at each developmental stage according to the saline doses.

Salinity dose	NRCT	NRCT	NRCT
	Tillering	Flowering	Grain filling
0EC	0.36 a	0.39 a	0.31 b
1EC	0.33 b	0.37 b	0.29 c
2EC	0.34 ab	0.37 b	0.31 b
3EC	0.35 a	0.37 b	0.33 ab
4EC	0.35 a	0.38 ab	0.34 a
VC (%)	3.02	2.49	2.82

Electrical conductivity- EC; 0EC- 0 dS m^{-1}; 1EC- 1dS m^{-1}; 2EC- 2dS m^{-1}; 3EC- 3 dS m^{-1}; 4EC- 4 dS m^{-1}; VC: coefficient of variation. Means followed by different letters are statistically different by Tukey's test ($p<0.05$).

At the tillering stage, the 0EC and 1EC doses presented the highest and lowest NRCT values, respectively, the latter not differing from 2EC (Table 3). The highest values at the beginning of flowering were observed for 0EC and 4EC, with no difference between salinity doses, and the lowest value was observed for 1EC at grain filling.

These results indicate that the negative effects of salt stress on rice depend not only on the salt dose but also on the sensitivity of the phenological growth stage to the dose. Elmetwalli et al. (2020) found that the usefulness of NRCT to assess soybean growth, yield, and water status depends on the irrigation level and growth stage. This distinct behavior is related to plant adaptation by regulating internal mechanisms, such as the storage of Na^+ ions inside the vacuole, with plants strongly reducing ionic toxicity, resisting salinity, and reducing cell damage (Bertazzinni et al., 2018; Roy et al., 2014) as an adaptation to saline stress, in which plants seek adjustment to ionic and osmotic stress (Sarkar et al., 2019).

Table 4 shows the interaction between salt doses and soil moisture for NRCT during harvest. A difference within moisture was observed only for the control treatment, but NRCT under moisture at field capacity presented a higher value than the moisture at saturation. It occurs because moisture at the saturation range presents a higher water volume available to the plants, keeping a more favorable absorption condition. Moisture did not interfere with the indices at the other doses. On the other hand, salt doses had inverse behavior within each moisture range: the highest NRCT values at FC and SAT were observed in the control and the highest dose (4 dS m^{-1}), respectively.

TABLE 4. The normalized relative canopy temperature (NRCT) index for the interaction between salinity doses and soil moisture content (field capacity-FC and saturate-SAT), during harvest.

	Salinity doses					
Soil moisture	0EC	1EC	2EC	3EC	4EC	VC (%)
FC	0.36 Aa	0.32 Ba	0.33 Ba	0.32 Ba	0.34 Ba	2.34
SAT	0.32 Bb	0.32 Ba	0.33 ABa	0.33 ABa	0.35 Aa	

Electrical conductivity- EC; 0EC- 0 dS m^{-1}; 1EC- 1dS m^{-1}; 2EC- 2dS m^{-1}; 3EC- 3 dS m^{-1}; 4EC- 4 dS m^{-1}; VC: coefficient of variation. Means followed by different lowercase letters in the column and uppercase letters in the row are statistically different by Tukey's test ($p<0.05$).

The highest NRCT values were found at the flowering stage, a period of highest sensitivity to salt and water stress of rice plants (Guimarães et al., 2016). The increase in the index during this stage may indicate physiological stress, compromising yield due to higher sterility of spikelets (Scivittaro et al., 2014) and early senescence, which shortens the grain filling stage, making them remain lighter and with a lower starch content (Prathap et al., 2019). Thus, resistance is acquired throughout the cycle, and NRCT decreases as the plant reaches the grain filling and harvesting stages.

The shoot fresh and dry mass values of the rice plants allowed the determination of the canopy water content (CWC), which was altered by soil moisture (Table 5). The difference between the two moisture ranges shows the plant water status, as expected in the treatments that received the highest irrigation depths (saturation).

TABLE 5. Canopy water content (CWC) according to soil moisture (field capacity-FC and saturate-SAT), during harvest.

Soil moisture	Canopy water content (%)
FC	63 b
SAT	65 a
VC (%)	3.63

VC: coefficient of variation. Means followed by different letters are statistically different by Tukey's test ($p<0.05$).

Low CWC indicates a reduced transpiration rate as a water-saving strategy, which results in higher leaf temperatures (Elsayed et al., 2017). This relationship was observed only at harvest for the 0EC dose (Table 4), as the other cultivation stage showed no effect of moisture on NRCT (Table 3).

Elsayed et al. (2015) identified severe (50% of irrigation depth) and mild (100% of irrigation depth) water stress conditions in barley cultivation, with NRCT values equal to 0.83 and 0.33, respectively. The index ranged from 0.73 to 0.42 (Elsayed et al., 2017), 0.71 to 0.26 (Elsayed et al., 2021), and 0.79 to 0.17 (Elmetwalli et al., 2020) for wheat, potato, and soybean, respectively, for an irrigation regime of 100, 75, and 50% of crop evapotranspiration.

In our study, the index ranged from 0.39 (flowering stage, 0EC) to 0.29 (grain filling stage, 1EC) during the cycle, regardless of the soil moisture. The irrigation depth at saturation was 64% higher than that of FC (Figure 4), but it did not influence NRCT, as observed by Elsayed et al. (2015), indicating that the stress found in this study is related to salinity and not to water availability.

Figure 5 shows the regression between NRCT and CWC. The best fit for the index behavior was the quadratic model. The NRCT value decreases while CWC increases to lower values up to 63% within the temperature range of this study. This result suggests an increase in the plant canopy water content, with a reduction in stress due to the transpiration effect, related to the higher water absorption by roots, leading to a reduction in canopy temperature and NRCT.

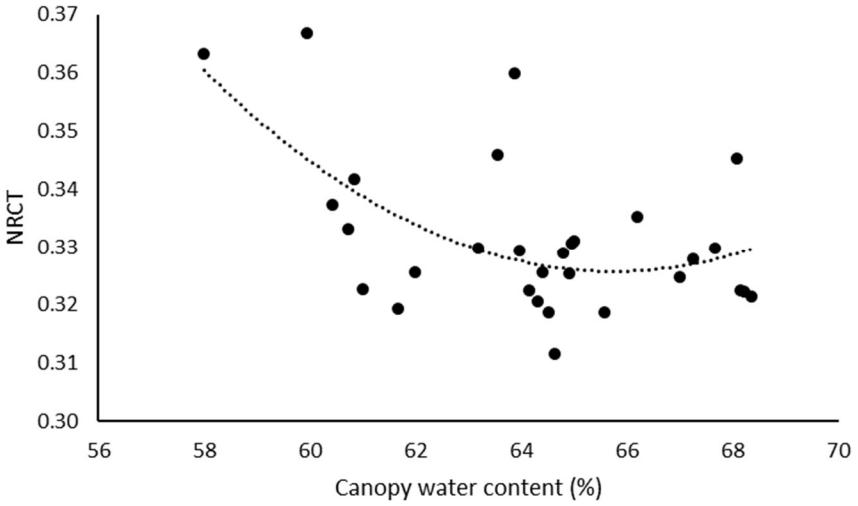

FIGURE 5. Regression curve of the normalized relative canopy temperature (NRCT) index and canopy water content (CWC) presented by the rice plants. NRCT values range between 0 and 1, with the most severe stress when the values are close to 1. R^2: 34%; NRCT = 2.82 – 0.0758 CWC + 0.0006 CWC^2.

However, the model (Figure 5) presented limitations for CWC values greater than 63%, indicating less water absorption and a slight increase in stress. The results suggest continuity of studies, aiming to expand the scale of soil moisture, as the minimum value of the adjustment corresponds to soil moisture at FC (Table 5). The inflection point of the curve is justified by the moisture effect on saturation (Table 5), with an increase in salinity in the solution (Table 1), verified by an increase in NRCT in the 4EC treatment relative to the control (Table 4).

CONCLUSIONS

The analysis of the electrical conductivity in the soil solution over time showed that soil moisture at field capacity concentrated the salts in the dripper moisture range, but with a dilution effect at saturation, although the volume of salts applied under this condition was higher.

The use of the algorithm in the processing of thermal images allowed the determination of the normalized relative canopy temperature (NRCT), which indicated the saline stress at the different development stages of arborio rice. The NRCT determination by thermal images showed higher sensitivity to saline stress at the flowering stage, showing a rebalance over time, confirmed at the grain filling and harvesting stages.

The assessment of the canopy water content (CWC) followed soil moisture (field capacity and saturation), as expected. The relationship between NRCT and CWC showed contradictory behavior, as the increase in canopy hydration increased the stress index, suggesting an influence of salinity on soil saturation conditions.

The results of this study provide insights into the importance of continuously monitoring saline stress during plant growth under saline irrigation regimes, using simple, low-cost approaches, such as thermal imaging. This information will be important in irrigation management in the context of water resource conservation both by reducing consumption and quality.

ACKNOWLEDGEMENTS

To São Paulo Research Foundation (FAPESP) for the research aid No. 2019/029212 and Coordenação de Aperfeiçoamento de Pessoal de Nível Superior – Brasil (CAPES) – Finance Code 001.

REFERENCES

Agam N, Cohen Y, Alchanatis V, Bem-Gal A (2013) How sensitive is the CWSI to changes in solar radiation? International Journal of Remote Sensing 34:6109-6120. DOI: https://doi.org/10.1080/01431161.2013.793873

ANA - Agência Nacional de Águas (2020). Mapeamento do arroz irrigado no Brasil. Brasília, ANA, 40 p.

Arai-Sanoh Y, Okamura M, Hosoi J, Nagata K, Takai T, Ogiwara H, Ishikawa J, Sakai H, Tokida T, Kobayashi N (2020) Yield response of high-yielding rice cultivar Oonari to different environmental conditions. Plant Production Science 23(1):69–74. DOI: https://doi.org/10.1080/1343943X.2019.1651207

Ayers RS, Westcot DW (1999) Water quality for agriculture. Rome, FAO. (Irrigation and Drainage paper, 29).

Bertazinni M, Sacchi GA, Forlani G (2018) A differential tolerance to mild salt stress conditions among six Italian rice genotypes does not rely on Na+ exclusion from shoots. Journal of Plant Physiology 226: 145–153.

Bheemanahalli R, Sathishraj R, Tack J, Nalley LL, Muthurajan R, Jagadish KSV (2016) Temperature thresholds for spikelet sterility and associated warming impacts for sub-tropical rice. Agricultural and Forest Meteorology 221: 122-130. DOI: https://doi.org/10.1016/j.agrformet.2016.02.003

Chapagain AK, Hoekstra AY (2011) The blue, green and grey water footprint of rice from production and consumption perspectives. Ecological Economics 70(4):749–758. DOI: https://doi.org/10.1016/j.ecolecon.2010.11.012

Coltro L, Marton LFM, Pilecco FP, Pilecco AC, Mattei LF (2017) Environmental profile of rice production in Southern Brazil: A comparison between irrigated and subsurface drip irrigated cropping systems. Journal of Cleaner Production 153: 491–505. DOI: https://doi.org/10.1016/j.jclepro.2016.09.207.

CONAB - Companhia Nacional de Abastecimento (2022) Acompanhamento da safra brasileira de grãos. Brasília, CONAB. v9, n4

Crusciol CAC, Fernandes AM, Carmeis Filho ACA, Alvarez RCF (2016) Macronutrient uptake and removal by upland rice cultivars with different plant architecture. Revista Brasileira de Ciência do Solo 40: e0150115. DOI: https://doi.org/10.1590/18069657rbcs20150115.

Elmetwalli AH, El-Hendawy S, Al-Suhaibani N, Alotaibi M, Tahir MU, Mubushar M, Hassan WM, Elsayed S (2020) Potential of Hyperspectral and Thermal Proximal Sensing for Estimating Growth Performance and Yield of Soybean Exposed to Different Drip Irrigation Regimes Under Arid Conditions. Sensors 20:6569. DOI: https://doi.org/10.3390/s20226569

Elsayed S, Rischbeck P, Schmidhalter U (2015) Comparing the performance of active and passive reflectance sensors to assess the normalized relative canopy temperature and grain yield of drought-stressed barley cultivars. Field Crops Research 177: 98–110. DOI: https://doi.org/10.1016/j.fcr.2015.03.010

Elsayed S, Elhoweity M, Ibrahim HH, Dewir YH, Migdadi HM, Schmidhalter U (2017) Thermal imaging and passive reflectance sensing to estimate the water status and grain yield of wheat under different irrigation regimes. Agricultural Water Management 189: 148–160. DOI: https://doi.org/10.1016/j.agwat.2017.05.001

Elsayed S, El-Hendawy S, Khadr M, Elsherbiny O, Al-Suhaibani N, Alotaibi M, Tahir MU, Darwish W (2021) Combining thermal and RGB imaging indices with multivariate and data-driven modeling to estimate the growth, water status, and yield of potato under different drip irrigation regimes. Remote Sensing 13(9):1679.

Ferreira DF (2019) SISVAR: A computer analysis system to fixed effects split plot type designs: Sisvar. Revista brasileira de biometria 37(4): 529-535.

Frukh A, Siddiqi TO, Khan MIR, Ahmad A (2020) Modulation in growth, biochemical atributes and proteome profile of rice cultivars under salt stress. Plant Physiology and Biochemistry 146: 55-70. DOI: https://doi.org/10.1016/j.plaphy.2019.11.011

Gerhards M, Schlerf M, Mallick K, Udelhoven T (2019) Challenges and future perspectives of multi-/Hyperspectral thermal infrared remote sensing for crop water-stress detection: A review. Remote Sensing 11(10): 1240.

Glenn DM (2012) Infrared and Chlorophyll fluorescence imaging methods for stress evaluation. HortScience 47(6): 697-698. DOI: https://doi.org/10.21273/HORTSCI.47.6.697

Guimarães CM, Stone LF, Silva ACDL (2016) Evapotranspiration and grain yield of upland rice as affected by water déficit. Revista Brasileira de Engenharia Agrícola e Ambiental 20(5):441–446. DOI: https://doi.org/10.1590/1807-1929/agriambi.v20n5p441-446

Idso SB, Jackson RD, Pinter Jr. PJ, Reginato RJ, Hatfield JL (1981) Normalizando o parâmetro estresse-grau-dia para a variabilidade ambiental. Meteorologia Agrícola 24:45-55

Jones HG, Serraj R, Loveys BR, Xiong L, Wheaton A, Price AH (2009) Thermal infrared imaging of crop canopies for the remote diagnosis and quantification of plant responses to water stress in the field. Functional Plant Biology 36: 978-989. DOI: https://doi.org/10.1071/FP09123

Khanal S, Fulton J, Shearer S (2017) An overview of current and potential applications of thermal remote sensing in precision agriculture. Computers and Electronics in Agriculture 139: 22-32. DOI: https://doi.org/10.1016/j.compag.2017.05.001

Khorsandi A, Hemmat A, Mireei SA, Amirfattahi R, Ehsanzadeh P (2018) Plant temperature-based indices using infrared thermography for detecting water status in sesame under greenhouse conditions. Agricultural Water Management 204: 222–233. DOI: https://doi.org/10.1016/j.agwat.2018.04.012

Kondo R, Tanaka Y, Katayama H, Homma K, Shiraiwa T (2021) Continuous estimation of rice (Oryza sativa (L.)) canopy transpiration realized by modifying the heat balance model. Biosystems Engineering 204: 294–303. DOI: https://doi.org/10.1016/j.biosystemseng.2021.01.016

Li F, Mistele B, Hu Y, Chen X, Schmidhalter U (2014) Reflectance estimation of canopy nitrogen content in winter wheat using optimised hyperspectral spectral indices and partial least squares regression. European Journal of Agronomy 52:198-209.

Liu Y, Hatou K, Aihara T, Kurose S, Akiyama T, Kohno Y, Lu S, Omasa K (2021) A robust vegetation index based on different UAV RGB images to estimate SPAD values of naked barley leaves. Remote Sensing 13(4): 686.

Mahlein AK, Rumpf T, Welke P, Dehne HW, Plümer L, Steiner U, Oerke EC (2013) Development of spectral indices for detecting and identifying plant diseases. Remote Sensing of Environment 128: 21-30.

Mekawy AMM, Assaha DVM, Yahagi H, Tada Y, Ueda A, Saneoka H (2015) Growth, physiological adaptation, and gene expression analysis of two Egyptian rice cultivars under salt stress. Plant Physiology and Biochemistry 87: 17-25. DOI: https://doi.org/10.1016/j.plaphy.2014.12.007

Prathap V, Kishwar A, Singh A, Vishwakarma C, Krishnan V, Chinnusamy V, Tyagi A (2019) Starch accumulation in rice grains subjected to drought during grain filling stage. Plant Physiology and Biochemistry 142: 440–451. DOI: https://doi.org/10.1016/j.plaphy.2019.07.027

Roy SJ, Negrão S, Tester M (2014) Salt resistant crop plants. Current opinion in biotechnology 26: 115-124. DOI: https://doi.org/10.1016/j.copbio.2013.12.004

Sánchez B, Rasmussen A, Porter JR (2014) Temperatures and the growth and development of maize and rice: a review. Global Change Biology 20:408-417. DOI: https://doi.org/10.1111/gcb.12389

Sarkar RK, Chakraborty K, Chattopadhyay K, Ray S, Panda D, Ismail AM (2019) Responses of rice to individual and combined stresses of flooding and salinity. In: Hasanuzzaman M et al. Advances in rice research for abiotic stress tolerance. Duxford, Woodhead Publishing. v13, p281-297. DOI: https://doi.org/10.1016/B978-0-12-814332-2.00013-7

Scivittaro WB, Silva GT, Lacerda CL, Neves WT, Corrêa GS, Farias MO (2014)Desempenho produtivo de genótipos de arroz irrigado sob estresse salino na fase reprodutiva. In: Reunião Sul-Brasileira de Ciência do Solo Fatos e Mitos em Ciência do Solo. Pelotas, NRS/SBCS.

Shanmugapriya P, Rathika S, Ramesh T, Janaki P (2019) Applications of remote sensing in agriculture-A Review. International Journal of Current Microbiology and Applied Sciences 8(1): 2270-2283.

Sharda R, Mahajan G, Siag M (2017) Performance of drip-irrigated dry seeded rice (Oryza sativa L.) in South Asia. Paddy Water Environment 15: 93-100. DOI: https://doi.org/10.1007/s10333-016-0531-5

Sidhu HS, Jat ML, Singh Y, Sidhu RK, Gupta N, Singh P, Singh P, Jat HS, Gerard B (2019) Sub-surface drip fertigation with conservation agriculture in a rice-wheat system: A breakthrough for addressing water and nitrogen use efficiency. Agricultural Water Management 216: 273–283. DOI: https://doi.org/10.1016/j.agwat.2019.02.019

Silva EFF (2002) Manejo da fertirrigação e controle da salinidade na cultura do pimentão utilizando extratores de solução do solo. Tese, Universidade de São Paulo, Escola Superior de Agricultura “Luiz de Queiroz”.

Sishodia RP, Ray RI, Singh SK (2020) Applications of remote sensing in precision agriculture: A review. Remote Sensing 12(19): 3136.

SOSBAI - Sociedade sul-brasileira de arroz irrigado (2018) Arroz irrigado:
recomendações da pesquisa para o Sul do Brasil. Cachoeirinha, SOSBAI, 205p.

Struthers R, Ivanova A, Tits L, Swennen R, Coppin P (2015) Thermal infrared imaging of the temporal variability in stomatal conductance for fruit tress. International Journal of Applied Earth Observation and Geoinformation 39: 9-17. DOI: https://doi.org/10.1016/j.jag.2015.02.006

van Genuchten MT (1980) A closed form equation for predicting the hydraulic conductivity of unsaturated soils. Soil Science Society of America Journal 44: 892-898.

van Genuchten MT, Leij FJ, Yates SR (1991) The RETC Code for Quantifying the Hydraulic Functions of Unsaturated Soils, EPA Report 600/2- 91/065, U.S. Salinity Laboratory, USDA-ARS, Riverside, California.

Zamann M, Shahidd SA, Heng L (2018) Guideline for salinity assessment, mitigation and adaptation using nuclear and related techniques. Switzerland, Springer Nature.